Sensors and Actuators: A. Physical 333 (2022) 113233

Contents lists available at ScienceDirect

Sensors and Actuators: A. Physical

journal homepage: www.elsevier.com/locate/sna

Analysis and evaluation of bundled SMA actuator wires

Rouven Britz[a,*], Paul Motzki[b]

[a] Department of Systems Engineering, Department of Materials Science and Engineering, Saarland University, Saarbrücken, Germany
[b] Center for Mechatronics and Automation Technologies (ZeMA gGmbH), Saarbrücken, Germany

ARTICLE INFO

Article history:
Received 25 June 2021
Received in revised form 29 October 2021
Accepted 16 November 2021
Available online 23 November 2021

Keywords:
Shape Memory Alloys
SMA
Bundle
Ni-Ti
NiTi
Nitinol
High Force
Actuator

ABSTRACT

The attractive properties of shape memory alloys (SMA), especially their high energy density, steadily expand the range of applications in which SMA wires represent attractive alternative actuator components. Industrial applications in particular, oftentimes require large forces, which scale with the diameter of SMA actuator wires. The higher the required actuator force, the larger the total effective cross-sectional area of the SMA wires is needed. Increasing the SMA wire diameter results in worse actuator dynamics due to a decreasing surface-to-volume ratio and thus slower convective cooling. Instead of simply increasing the wire diameter, the bundling of several thin wires offers a suitable alternative to generate higher forces. This results in an increased surface-to-volume ratio and thus permits higher dynamic system performance.

This paper discusses the mechanical and thermal behavior of SMA wire bundles and shows the influence of contact resistance inside the clamps, which is important to optimize for a long-lasting functionality of SMA bundles. In addition, the experiments show an indirect heating between single SMA wires inside a bundle, which leads to an energy saving capability up to 60%. Two electro-mechanical experiments show the behavior of SMA bundles in a constant force and a constant strain measurement. The experimental results show a maximum stroke of 4–4.5% and a generated maximum force of 1200 N. The results are discussed to provide an understanding of the mechanical characteristics of SMA bundles. In addition, an infrared (IR)-Camera provides an insight into the thermal behavior.

1. Introduction

Shape memory alloys (SMAs) are well known for bio-medical applications like stents or guide wires [1–6]. Recently, SMA research is focusing on the high potential as lightweight integrated actuator systems [7–19], as well as the strongly emerging field of elastocaloric cooling [20–23]. Due to their high energy density and multi-functional properties [24], they are suitable for the design of compact actuator-sensor-systems. In the automotive sector and consumer electronics, SMA based actuator systems have already established in several applications [25–29]. Typically, nickel-titanium (NiTi) actuator wires with a diameter between 0.025 mm and 0.5 mm are used [30,31] as SMA actuators. The thermal shape memory effect as underlying effect of shape memory actuators is based on a reversible phase transformation of the material crystal lattice between the low temperature martensitic phase and the high temperature austenitic phase. The cold wire elongates when a tensile stress is applied. Joule heating by an electric current lead to a temperature increase of the wire, which results in a macroscopic contraction. Microscopically, the length change is based on a first order phase transformation from the martensitic lattice structure to the austenitic lattice [24], [32]. After the wire is cooled down, an external force can return the wire to its original length. This process is thus repeatable. The contraction of the wire can be correlated with the electrical resistance of the wire, referred to as “self-sensing” effect [33].

Actuator systems using SMA technology usually consist of an SMA element and a biasing mechanism like a spring or a mass. The diameter of the SMA wire is determined by the required force. A higher force means a larger diameter accompanied by reduced system dynamics. Using multiple SMA wires in parallel allows for generating high forces without decreasing the dynamic performance, as shown in a bistable SMA vacuum suction cup [34]. In contrast to an SMA bundle in form of a twisted cable, which makes a convective cooling of the single wires almost impossible, a bundle of separated wires allows an airflow through the bundle and therefore improved convective cooling for better dynamic behavior.

Since an SMA bundle consists of several SMA wires arranged mechanically parallel, the actuator can compensate the breakdown of a single wire. Thus, bundling SMA wires not only allows for a high output force system with a high dynamic performance, but also provides an increased reliability and redundancy. A major challenge

* Corresponding author.
E-mail address: rouven.britz@imsl.uni-saarland.de (R. Britz).

https://doi.org/10.1016/j.sna.2021.113233

when using SMA wires as actuators is the electrical integration and contacting. There are basically two ways to contact the SMA wires electrically within a bundle - in series or in parallel configuration. The following example is intended to briefly illustrate the advantages and disadvantages of the two electrical configuration options and their effects on the mechanical properties.

An exemplary NiTi SMA wire with a diameter of 0.25 mm and a length of 100 mm has a resistance of approximately 1.85 Ω. To heat the wire up to the austenite finish temperature of 90 °C, a current of 1050 mA for 1 s at 172 MPa mechanical tensile stress is needed [30]. A voltage of 1.94 V is required to generate this current flow through the wire. Contacting five wires in series, the voltage increases to 9.7 V, because of the resistance increase by a factor of five. The failure of a single SMA wire in a serially contacted bundle would result in an overall actuator system failure. The insulation of the wires to each other and inside the clamps is also critical in the serial case since short circuits lead to inactive areas of the bundle. Contacting the SMA electrically in parallel, a current of 5.25 A is required, since the resistance is reduced by a factor of five, while the voltage drop remains at 1.94 V. The disadvantage of the high current flow using this topology can be compensated by the mechanical advantages. The system is mechanically redundant. Contrarily to the arrangement of the SMA wires in series, the failure of a single wire does not lead to an actuator failure. Such a defect can be easily detected by a resistance measurement and the actuator bundle can be replaced during planned maintenance. Additionally, a lower design effort is required since no electrical insulation in between the SMA wires is required.

In this paper, SMA bundles in electrical parallel configuration are investigated. First, the experimental setup to characterize SMA bundles in different power and load conditions will be presented. The setup includes an IR-Camera to determine the thermal characteristics of the SMA bundles, including the temperature distribution of an SMA bundle in general as well as the influence of the clamps on it. Also, a possible thermal influence of a wire to each other wires in the bundle can be observed by the IR-Camera. After outlining the thermal measurements, the experiments to characterize the mechanical and electrical behavior of parallel SMA bundles are discussed. The results show a significant mutual influence of the wires in a bundle, which can help save energy. The findings of the possibilities of an SMA bundle in terms of force, stroke, electrical properties and energy saving will subsequently serve as a basis for the design of future actuator-sensor systems based on bundled SMA actuator wires.

2. Materials and methods

The measurement setup is based on components from National Instruments and uses LabVIEW to control the experiments and record the data. A load cell KS25 from GTM is attached to measure the generated force of the SMA bundle, while a linear drive – in combination with a control algorithm – allows either holding a constant stress level of the SMA bundle during activation for constant force measurements or a constant position for constant strain measurements. In both cases, the SMA bundle voltage and current are measured with a NI CompactRIO data acquisition system. The voltage is measured by a NI 9229 voltage measuring module, the current by a NI 9227 current measuring module. Additionally, an IR-Camera IR 8380 from Infratec is equipped, enabling for the measurement of the temperature distribution of the bundles. Fig. 1, right shows the vertically arranged final experimental setup including an SMA bundle.

The SMA bundles are made of commercially available SMA wires. Due to a standardized manufacturing process, reproducible properties of the SMA material are given and documented by the manufacturer in [36]. Fig. 2 shows a DSC measurement of the used SMA material.

3. Results

3.1. Thermal investigations

In this section, the results of the thermal investigations of SMA wire bundles are presented and discussed. In this study, two bundles of different sizes are compared. The first bundle consists of four wires mechanically in parallel and the second bundle analogously of 28 wires. In general, heating an SMA wire yields a phase transformation and thus a force can be generated. The force that can be generated by one wire and thus the mechanical stress in the material depends on the temperature of the wire. Therefore, a homogeneous

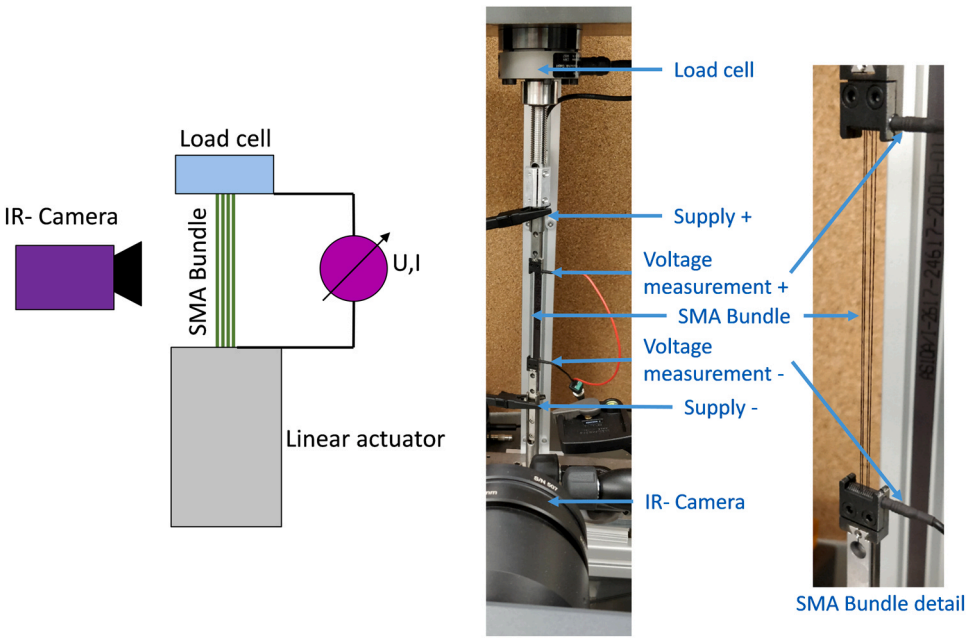

Fig. 1. Schematic view of the test rig (left) and final experimental setup with SMA bundle (right) [35].

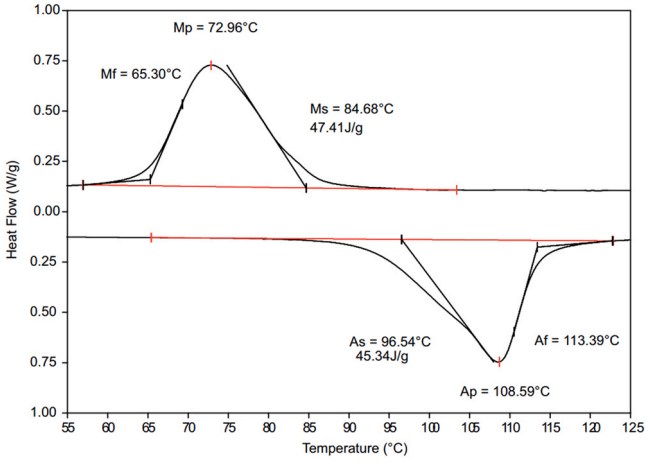

Fig. 2. DSC measurement of the used SMA material [36].

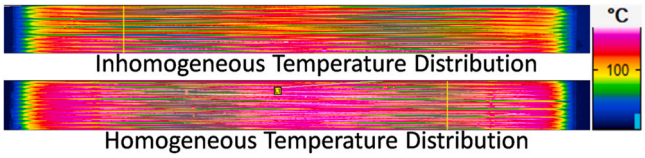

Fig. 3. Inhomogeneous (upper part) and homogeneous (lower part) temperature distribution of an SMA bundle.

temperature distribution and hence equal temperatures in all wires is inevitable for an actuation using SMA bundles to ensure an equal load distribution over all wires and to avoid an overload of single wires. The upper part in Fig. 3 shows an IR-Camera recording, where an inhomogeneous temperature distribution can be observed. The bundle is divided into two temperature areas, a hotter section at the bottom (pink) and a colder section at the top (red and yellow, respectively). Such an inhomogeneous temperature distribution suggests different Joule heating of the single wires. The Joule heating depends on the electrical power, which is influenced by the current through the wires and their electrical resistance. But since all SMA wires have through a semi-automatic winding process, which keeps the pretension constant, initially the same dimensions, phase configuration and temperature, their resistance is also identical. This leads to the conclusion that the contact resistance inside the clamps has an important influence on the current flow. By adding copper foil and silver paste inside the clamps a better contact resistance could be ensured and thus a homogeneous temperature distribution is achieved (Fig. 3, lower part).

Looking at the temperature of individual wires in the bundle over time using a measurement line at one position on the x-axis (Fig. 4), a temperature gradient from the inner wires to the outer wires can be observed. The pictures of the IR-Camera show only one half of the SMA wires of a bundle, since the bundles are arranged in two layers (see Fig. 1: SMA Bundle detail). As a consequence, only the front layer of the bundle is observed, for example 14 SMA wires while investigating a bundle of 28 SMA wires.

The temperature distribution in Fig. 4 has two reasons: On the one hand, there is a better heat exchange of the outer wires with the environment, on the other hand, there is reduced indirect heating of these outer wires by less adjacent wires. Indirect heating means a heat exchange from one wire to another through the air gap between them. The measurement shows a significant heating of the air between the wires, in contrast to Fig. 5 with an insulating layer of air between the wires. In both experiments, the energy per wire is identical. The two bundles with four and 28 wires respectively, differ regarding the resulting maximum temperature. Figs. 4 and 5 show the two measurements and a lower maximum temperature in the wires of the bundle with four wires can be observed. This indicates a higher heat transfer to the environment and therefore a decrease in the temperature of the bundles. With increasing temperature between the single wires, the temperature gradient between a wire and the surrounding air decreases, which in turn helps heating up the wires. The influences of this effect regarding actuation properties are described in the experiments in Section 4.

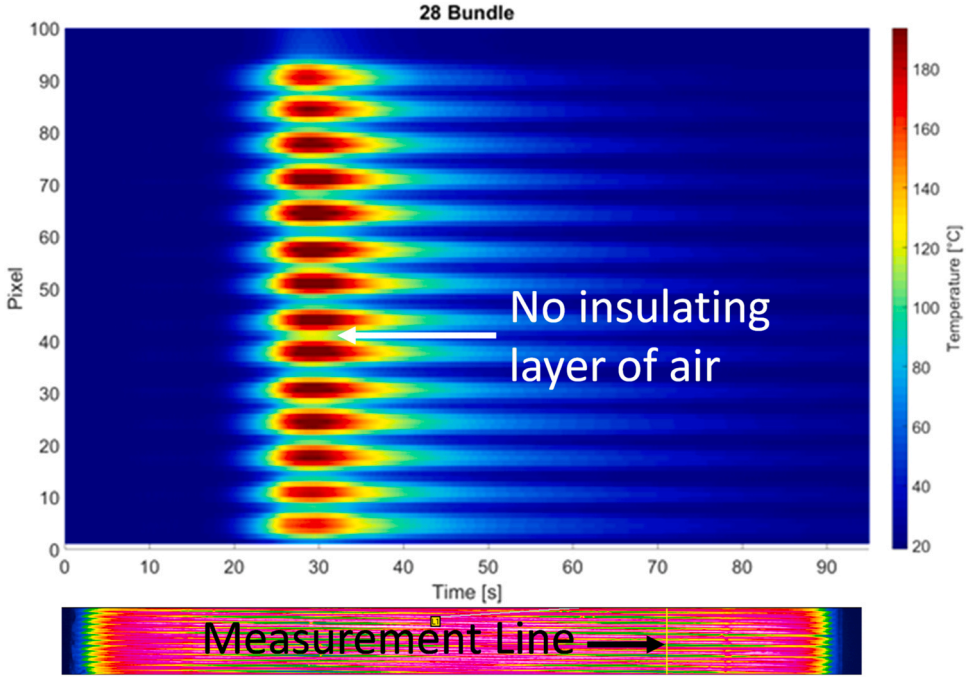

Fig. 4. Temperature distribution inside a bundle of 28 wires [35].

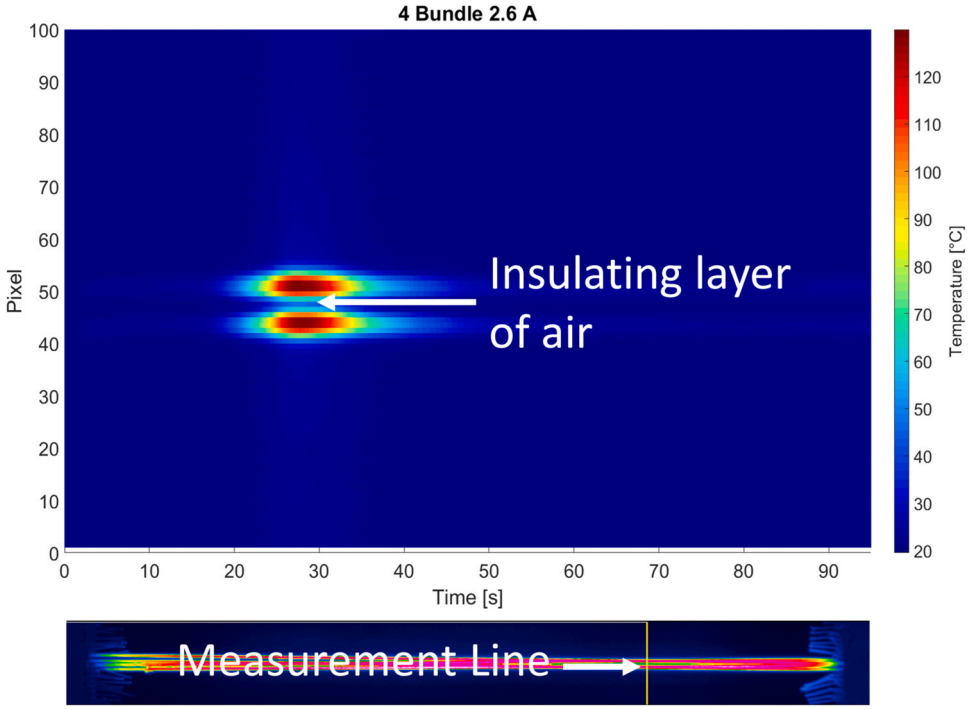

Fig. 5. Temperature distribution inside a bundle of 4 wires [35].

3.2. Constant force and constant stroke measurements

This section discusses the electro-mechanical measurements of SMA bundles using SMA wires with a diameter of 250 µm and a length of 100 mm. The total dimensions of the bundles including the clamps are 130 mm of length and 16 mm of width (Fig. 6).

To characterize their mechanical behavior by an electrical activation, two experiments are conducted, representing two extreme stress types (maximum stroke and maximum force) of SMA wires. In the first experimental series, the bundles are loaded with a constant force while being activated. As a result of these experiments the maximum stroke of the SMA bundle is obtained. In the second series of experiments, the bundle is pre-strained to a defined stress level. After reaching this stress level, the position is fixed, while the SMA wires are activated. As a result, the maximum (blocking) force of the SMA bundle is obtained.

Seven different bundle types with SMA wire numbers between four and 28 are used for the following measurements.

3.2.1. Constant force experiment results

The constant force experiments show the maximum stroke of the SMA bundles. Each bundle is loaded with a force equivalent to a mechanical pre-stress of 200 MPa per wire (Fig. 7a) and this load is kept constant during the experiment. An electrical current in triangle signal form with a rising and falling time of 90 s each is applied to activate the wires. The peak of each current triangle is predetermined and corresponds to a peak current of 0.39 A per wire, assuming a homogeneous current distribution (Fig. 7d). A homogeneous current distribution leads to a homogeneous temperature distribution, which leads to a homogeneous load distribution and prevents overloads.

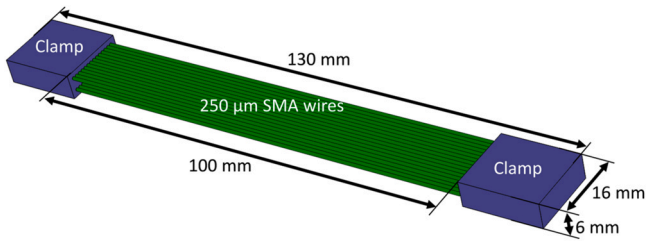

Fig. 6. Sketch of the SMA bundle dimensions.

The wires contract up to a maximum value of 4 mm, which corresponds to a stroke of 4% (Fig. 7b,c). The voltage signals in Fig. 7e show significant changes in the voltage rise rate at 80 – 90 s with the exception of the bundle of 4 wires, which shows an almost constant voltage rise rate. The voltage drop over the wires is influenced by the electrical resistance of the wires, which is described by the equation [37]:

$$R_{SMA}(T, x_A, x_+, x_-) = \rho_{SMA}(T)\frac{L}{A} \tag{1}$$

with

$$\rho_{SMA}(T) = x_+\rho_+(T) + x_-\rho_-(T) + x_A\rho_A(T) \tag{2}$$

The equation shows that three factors contribute to the resistance of SMA wires: The temperature T, the phase fractions x_A, x_+, x_- and the wire geometry, where L is length of the wire and A is the cross-sectional area. Fig. 8 (left upper part) shows the bundle resistance as a function of time calculated with the measured voltage and current. Fig. 8 (right upper part) shows the bundle resistance as a function of temperature. The resistance of the bundles decreases according to the equation for parallel connection of resistors:

$$\frac{1}{R_{Total}} = \sum_{i=1}^{n}\frac{1}{R_i} \tag{3}$$

For example, with a resistance of 18.5Ω/m [30] for a 250 µm wire and a length of 100 mm, one wire has a theoretical resistance of 1.85Ω. A bundle of 4 wires has a total resistance of 0.46Ω (Eq. 3).

For better comparison of the resistance behavior, the specific resistance is calculated and shown in Fig. 8 (lower part). It is shown

that the resistance drop decreases with a decreasing number of wires. The lower resistance change correlates with the lower stroke shown in Fig. 7b.

The reason for this lower resistance change is shown in Fig. 9, illustrating the temperature of the bundles over time. To measure the temperature of the wires, again the IR-Camera is used. The maximum temperature of the bundle with four wires is less than 90 °C, thus below the austenite finish temperature. Due to this low temperature, there is only little phase transformation and therefore low wire contraction. Although the current per wire is equivalent in all experiments, the heating rate decreases with a decreasing number of wires in the bundle. This indicates a lower indirect heating by the adjacent wires and results in the lower maximum temperature. The plateaus in the temperature measurement at 75 and 175 s indicate the latent heat that is absorbed or released during the phase transformation. The maximum temperature of the wires in the bundle with four wires and in the bundle of eight wires is too low to develop such a plateau, indicating only a small amount of phase transformation.

To compensate the low indirect heating, more active heating is required to achieve the same stroke of 4–4.5%. For this purpose, a second experiment with the bundle of 4 wires is conducted by increasing the current peak in 0.5 A steps, from 1.6 A to 2.6 A. The result of the stroke measurement at different peak currents is shown in Fig. 10 (upper part). After an increase of 1 A the stroke reaches 4–4.5%. The delta of the resistance (Fig. 10, lower part) increases as well, which indicates a near full phase transformation.

The calculation of the energy input per wire shows nearly the same energy levels in the first experiment for all bundles (see Fig. 11, green lines). As shown, the bundle of four wires only contracts about 1% at this energy level. The performance of such a bundle can be improved using a higher energy input (Fig. 11, red and orange lines). A bundle of 28 SMA wires saves more than 60% of the energy in contrast to the bundle with four wires assuming a complete

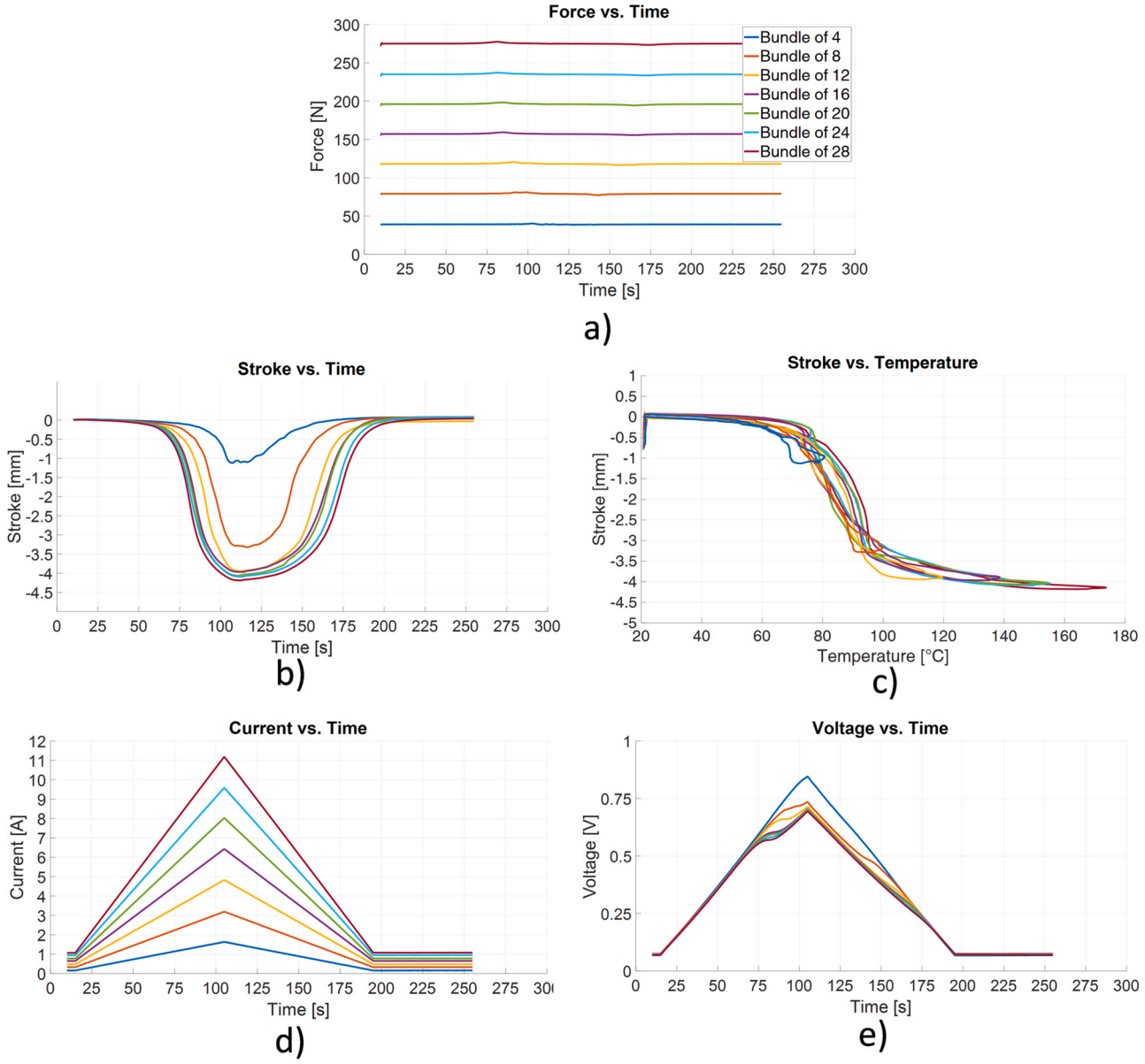

Fig. 7. Measured data from the constant force experiment – a) constant force of each bundle equivalent to a mechanical pre-stress of 200 MPa per wire, b) resulting stroke of each bundle due to activation over time, c) resulting stroke of each bundle due to activation over temperature, d) current triangle for activation, e) voltage drop over each bundle.

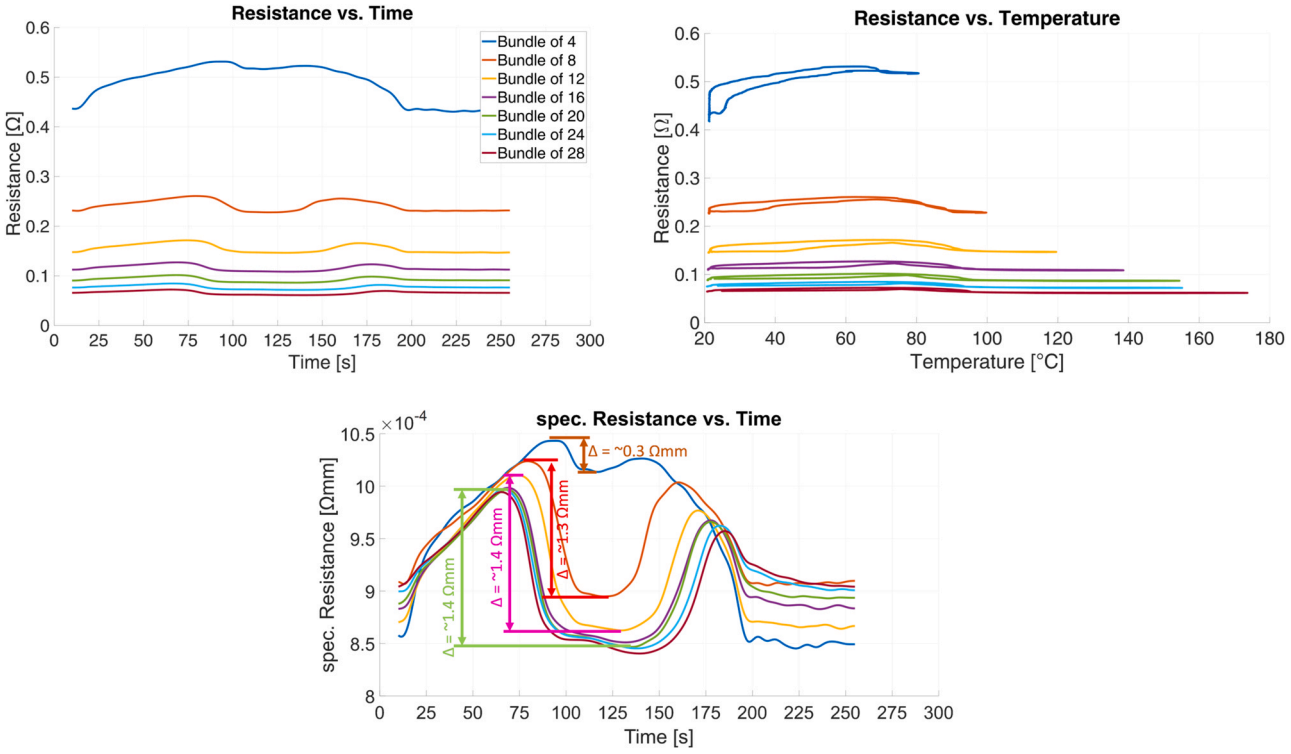

Fig. 8. Calculated resistance over time (left upper part), calculated resistance over temperature (right upper part) and specific resistance (lower part) of the SMA bundles in the constant force series of experiments.

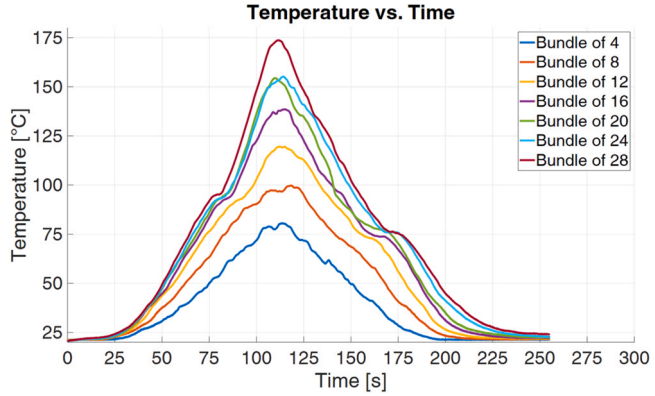

Fig. 9. Maximum temperature of SMA bundles in constant force experiment.

contraction of both bundles (Fig. 11). A bundle of multiple SMA wires not only brings the advantages mentioned, e.g. redundancy and high forces combined with increased dynamics, but it also helps to realize more energy-efficient activation.

3.2.2. Constant stroke experiment results

To complete the mechanical and electrical investigations of bundled SMA wires, a further series of experiments is conducted, pointing out the forces, which can be generated while using compact SMA bundle actuators. Each bundle is loaded to a force equivalent to a pre-stress of 200 MPa per wire. In contrast to the first experiment, the stroke is kept constant during the experiment (Fig. 12a). A current triangle with a rising and falling time of 10 s is applied to activate the wires. The peak of each current triangle is predetermined and corresponds to a peak current of 0.65 A per wire, assuming a homogeneous current distribution (Fig. 12d).

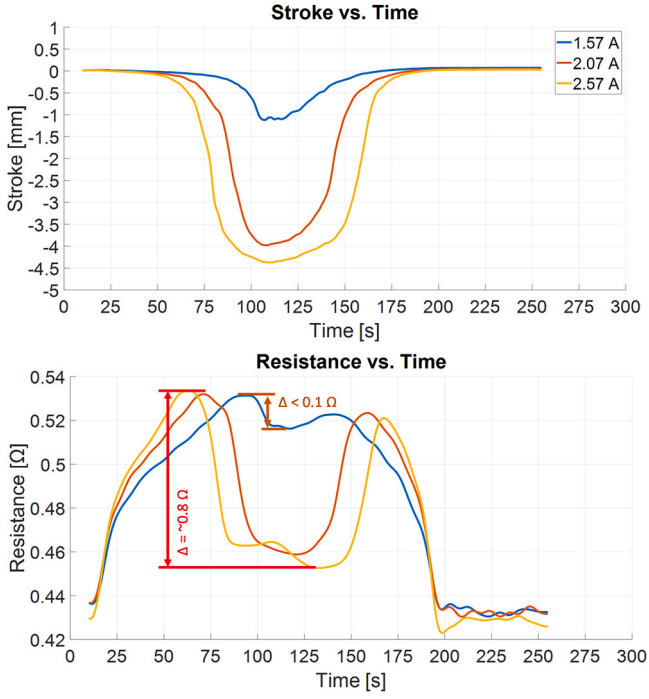

Fig. 10. Stroke (upper part) and resistance (lower part) change of a bundle of 4 wires by different currents.

Fig. 12b shows the resulting force due to the heating as a function of time. Each force maximum represents a stress maximum of about 850–900 MPa per wire, except the bundle of four wires with 700 MPa. Fig. 12c shows the resulting force due to the heating as a function of temperature. In this experiment, no voltage drops are visible in Fig. 12e, indicating less phase transformations. Plotting the

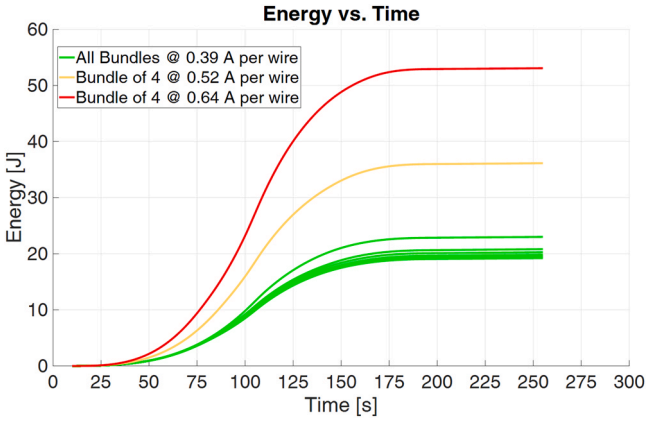

Fig. 11. Energy input for each wire in different experiments.

resistance as a function of time (Fig. 13, left upper part), and for a better comparison the specific resistance (Fig. 13, lower part), shows an equivalent behavior of the resistance like the temperature. Fig. 13 (right upper part) shoes the resistance as a function of temperature. First, the electrical resistance increases with increasing temperature, as it is typical for metal. First a sharp rise and after 16 s the resistance change rate changes until the temperature maximum at 28 s. This change indicates the phase transformations and generating the force, in contrast to the first experiment, the wire cannot transform to austenite completely. The constant increase of the mechanical stress results in an increase of the transformation temperature, so the transformation can only happen bit by bit.

The low generation of force of the bundle with four wires results from the low maximum temperature (Fig. 14). As already seen in the constant force experiments, this lower maximum temperature results from increased heat exchange to the environment compared to the heat exchange between the SMA wire themselves. Increasing the

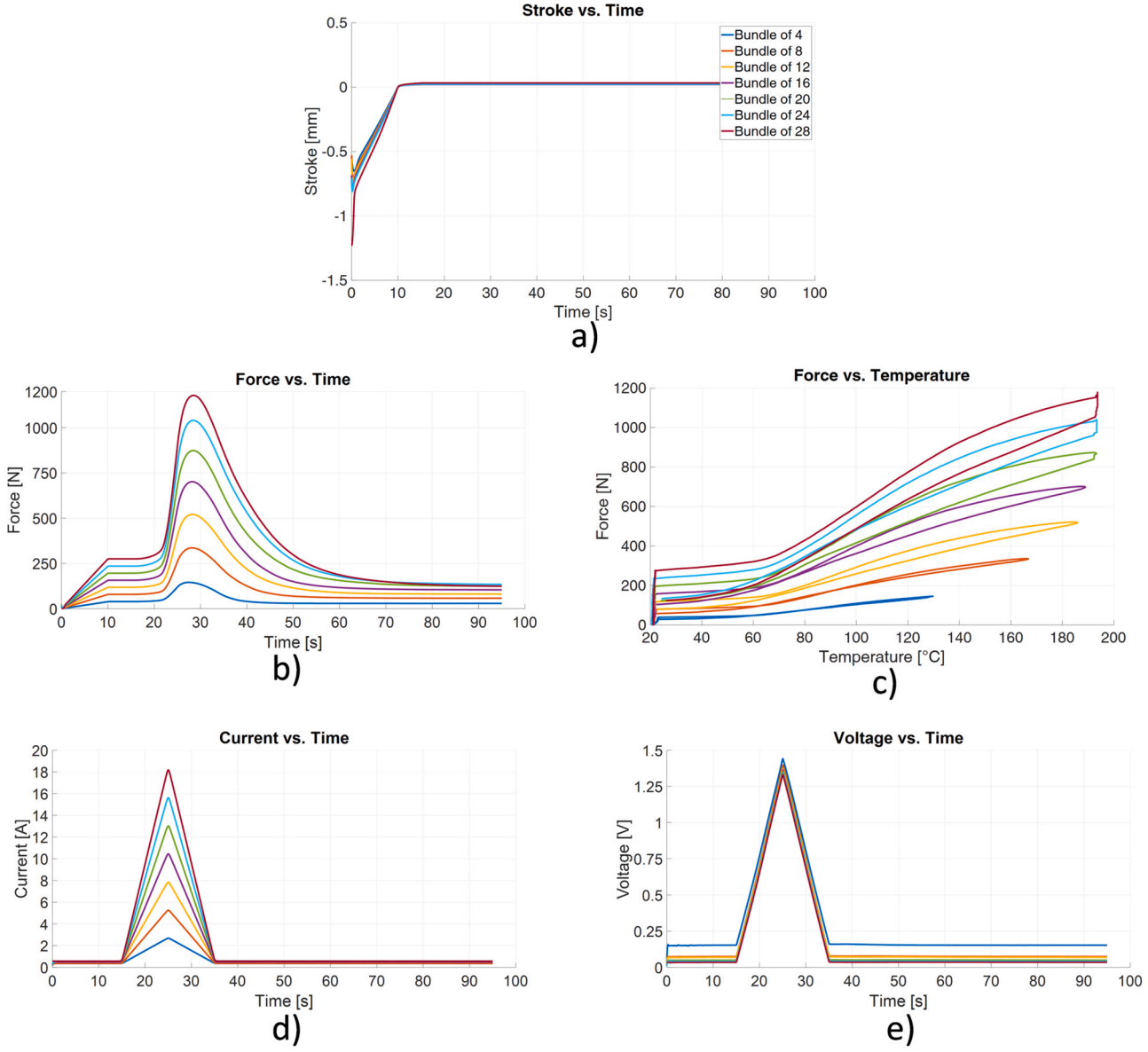

Fig. 12. Measured data from the constant stroke experiment – a) constant stroke of each bundle loaded to a mechanical pre-stress of 200 MPa per wire, b) resulting force of each bundle due to activation over time, c) resulting force of each bundle due to activation over temperature, d) current triangle for activation, e) voltage drop over each bundle.

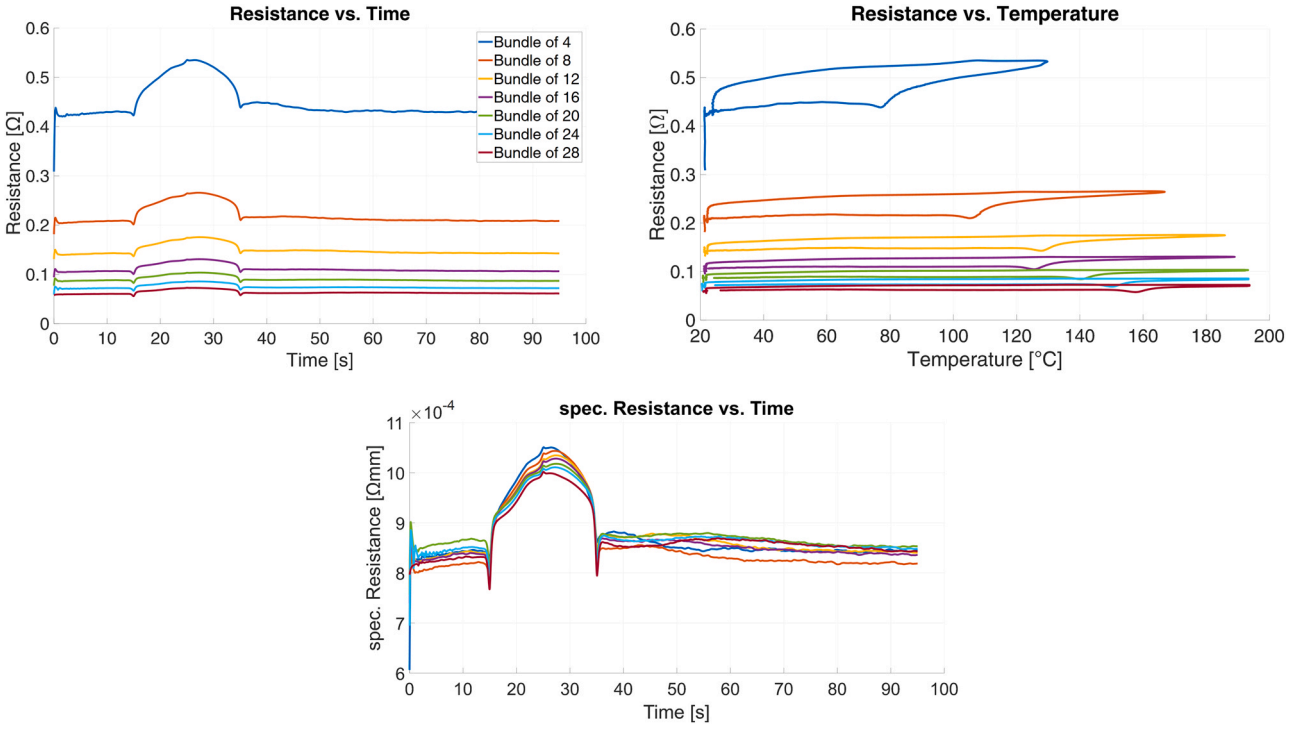

Fig. 13. Calculated resistance over time (left upper part), calculated resistance over temperature (right upper part) and spec. resistance (lower part) of SMA bundles in constant stroke experiments.

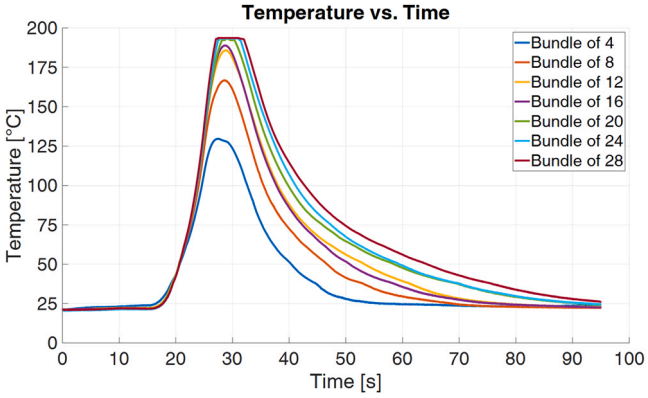

Fig. 14. Maximum temperature of SMA bundles in constant stroke experiments.

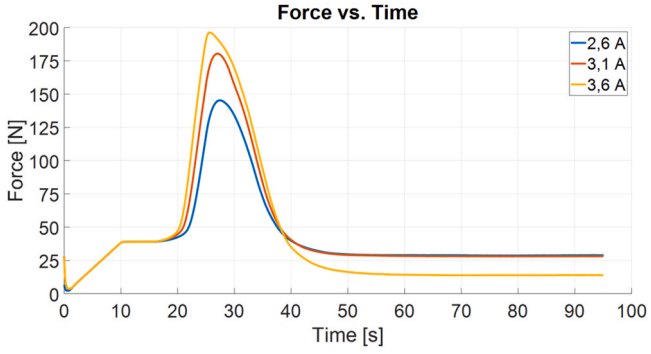

Fig. 15. Force change of a bundle of 4 wires by different currents.

current through the SMA wires can compensate for this behavior (Fig. 15).

4. Conclusion and outlook

First results of experiments with electrical and mechanical parallel SMA bundles have been presented. An overview of the advantages and disadvantages in contrast to an electrical series configuration has been outlined first. Subsequently, the test rig, enabling temperature measurements, as well as electrical-mechanical measurements, has been introduced. Section three discusses the thermal measurements of different SMA bundles, pointing out the importance of a low-ohmic contact resistance as well as the influence of the indirect heating between single SMA wires inside a bundle. Because of this indirect heating, up to 60% of the energy can be saved during activation. In section four, two series of experiments are presented, characterizing the mechanical and electrical behavior of SMA bundles. In the first series of experiments, the SMA bundles are loaded with a constant force. The experiment shows the resulting stroke of SMA bundles at constant loads. A maximum stroke of 4–4.5% can be obtained. In the second series of experiments, the stroke is kept constant. These experiments show the ability of generating high forces with compact SMA bundle actuators. A bundle of 28 SMA wires with a diameter of 250 µm is able to generate a maximum force of 1200 N.

In future work the influence of the distance between the wires will be investigated in order to optimize the energy savings due to indirect heating effects, which is in conflict with the cooling behavior and thus the desired high dynamics of SMA bundles. Due to the better surface-to-volume ratio, SMA bundling should results in an improved cooling behavior in comparison to one comparable thick SMA wire. Further investigations will show whether, in order to exploit this effect, the convection of the air is sufficient or whether an additional air flow is indispensable to get the warm air out of the bundle. In addition, effects like cumulative heating at repeated activation and the effects of mechanical pre-load and environmental conditions are important studies for future work. With these findings about SMA bundles, compact SMA actuators generating high forces at high frequencies can be specifically designed.

Declaration of Competing Interest

The authors declare that they have no known competing financial interests or personal relationships that could have appeared to influence the work reported in this paper.

References

[1] J. Mohd Jani, M. Leary, A. Subic, M.A. Gibson, A review of shape memory alloy research, applications and opportunities, Mater. Des. 56 (2014) 1078–1113, https://doi.org/10.1016/j.matdes.2013.11.084

[2] N.B. Morgan, Medical shape memory alloy applications - The market and its products, Mater. Sci. Eng. A 378 (1–2 SPEC. ISS) (2004) 16–23, https://doi.org/10.1016/j.msea.2003.10.326

[3] R. Pfeifer, C.W. Müller, C. Hurschler, S. Kaierle, V. Wesling, H. Haferkamp, Adaptable orthopedic shape memory implants, Procedia CIRP 5 (2013) 253–258, https://doi.org/10.1016/j.procir.2013.01.050

[4] S. Pittaccio, L. Garavaglia, C. Ceriotti, F. Passaretti, Applications of shape memory alloys for neurology and neuromuscular rehabilitation, J. Funct. Biomater. 6 (2) (2015) 328–344, https://doi.org/10.3390/jfb6020328

[5] K. Yanagihara, H. Mizuno, H. Wada, S. Hitomi, Tracheal stenosis treated with self-expanding nitinol stent, Ann. Thorac. Surg. 63 (6) (1997) 1786–1789, https://doi.org/10.1016/S0003-4975(97)00369-X

[6] I. Vinograd, B. Klin, T. Brosh, M. Weinberg, Y. Flomenblit, Z. Nevo, A new intratracheal stent made from nitinol, an alloy with 'shape memory effect, J. Thorac. Cardiovasc. Surg. 107 (5) (1994) 1255–1261, https://doi.org/10.1016/S0022-5223(94)70046-X

[7] P. Motzki and S. Seelecke, Bistable actuator device having a shape memory element, WO 2017/194591 A1, 2016.

[8] P. Motzki, F. Khelfa, L. Zimmer, M. Schmidt, S. Seelecke, Design and validation of a reconfigurable robotic end-effector based on shape memory alloys, ASME Trans. Mechatron. 24 (1) (2019) 293–303, https://doi.org/10.1109/TMECH.2019.2891348

[9] D.J. Hartl, D.C. Lagoudas, Aerospace applications of shape memory alloys, Proc. Inst. Mech. Eng. Part G J. Aerosp. Eng. 221 (4) (2007) 535–552, https://doi.org/10.1243/09544100JAERO211

[10] M. Kohl, Shape Memory Microactuators, Springer Verlag, Berlin Heidelberg, 2004.

[11] C. Lexcellent, Shape-memory Alloys Handbook. 2013.

[12] F. Simone, G. Rizzello, S. Seelecke, P. Motzki, A soft five-fingered hand actuated by shape memory alloy wires: design, manufacturing, and evaluation, Front. Robot. AI 7 (608841) (2020) 608841, https://doi.org/10.3389/frobt.2020.608841

[13] P. Motzki, S. Seelecke, Industrial applications for shape memory alloys, Reference Module in Materials Science and Materials Engineering, Elsevier, 2019.

[14] G.S. Mammano, E. Dragoni, Design and characterization of a continuous rotary minimotor based on shape-memory wires and overrunning clutches1, J. Mech. Des. 139 (1) (2016) 15001–15009, https://doi.org/10.1115/1.4034401

[15] O. Benafan, J. Brown, F.T. Calkins, P. Kumar, A.P. Stebner, T.L. Turner, R. Vaidyanathan, J. Webster, M.L. Young, Shape memory alloy actuator design: CASMART collaborative best practices and case studies, Int. J. Mech. Mater. Des. 10 (1) (2014) 1–42, https://doi.org/10.1007/s10999-013-9227-9

[16] J. Luntz, B. Barnes, D. Brei, P.W. Alexander, A. Browne, N.L. Johnson, SMA Wire Actuator Modular Design Framework, Proc. SPIE - Int. Soc. Opt. Eng. (2009), https://doi.org/10.1117/12.816752

[17] S.D. Oehler, D.J. Hartl, R. Lopez, R.J. Malak, D.C. Lagoudas, Design optimization and uncertainty analysis of SMA morphing structures, Smart Mater. Struct. 21 (2012) 094016, https://doi.org/10.1088/0964-1726/21/9/094016

[18] Y. Fu, H. Du, W. Huang, S. Zhang, M. Hu, TiNi-based thin films in MEMS applications: a review, Sens. Actuators A Phys. 112 (2–3) (2004) 395–408, https://doi.org/10.1016/j.sna.2004.02.019

[19] Y. Furuya, H. Shimada, Shape memory actuators for robotic applications, Mater. Des. (1991), https://doi.org/10.1016/0261-3069(91)90088-L

[20] M. Schmidt, S.-M. Kirsch, S. Seelecke, A. Schütze, Elastocaloric cooling: from fundamental thermodynamics to solid state air conditioning, Sci. Technol. Built Environ. 22 (5) (2016) 475–488, https://doi.org/10.1080/23744731.2016.1186423

[21] M. Schmidt, A. Schütze, S. Seelecke, Scientific test setup for investigation of shape memory alloy based elastocaloric cooling processes, Int. J. Refrig. 54 (2015) 88–97, https://doi.org/10.1016/j.ijrefrig.2015.03.001

[22] S. Qian, Y. Geng, Y. Wang, J. Ling, Y. Hwang, R. Radermacher, I. Takeuchi, J. Cui, A review of elastocaloric cooling: materials, cycles and system integrations, Int. J. Refrig. 64 (2016) 1–19, https://doi.org/10.1016/j.ijrefrig.2015.12.001

[23] J. Frenzel, G. Eggeler, E. Quandt, S. Seelecke, M. Kohl, High-performance elastocaloric materials for the engineering of bulk- and micro-cooling devices, MRS Bull. 43 (4) (2018) 280–284, https://doi.org/10.1557/mrs.2018.67

[24] H. Janocha, Unkonventionelle Aktoren - Eine Einführung, Oldenburg Verlag, München, 2010.

[25] D. Stoeckel, Shape Memory Actuators for Automotive Applications, 1990.

[26] J.B. Gault et al., Locking Mechanism, US 10,331,175 B2, 2019.

[27] "Ingpuls GmbH - Produktportfolio, 2020.

[28] M. Köpfer, Industrialisierung der FGL-Technologie in hochvolumigen Serienprodukt, VDI-Expertenforum: Smart Materials – aus der Forschung in die industrielle Anwendung. Karlsruhe, 2017.

[29] Actuator Solutions GmbH and A. S. GmbH, Actuator Solutions SMA Products, 2018.

[30] Dynalloy Inc, Technical Characteristics of Flexinol Actuator Wires, Dynalloy Inc., 2016, ⟨http://www.dynalloy.com/pdfs/TCF1140.pdf⟩.

[31] SAES Getters, SmartFlex Brochure, 2017.

[32] J. Van Humbeeck, M. Chandrasekaran, L. Delaey, Shape memory alloys: materials in action, Endeavour 15 (4) (1991), https://doi.org/10.1016/0160-9327(91)90119-V

[33] N. Lewis, A. York, S. Seelecke, Experimental characterization of self-sensing SMA actuators under controlled convective cooling, Smart Mater. Struct. 22 (9) (2013) 094012, https://doi.org/10.1088/0964-1726/22/9/094012

[34] S.-M. Kirsch, F. Welsch, M. Schmidt, P. Motzki, and S. Seelecke, Bistable SMA Vacuum Suction Cup, 2018.

[35] R. Britz et al., SMA wire bundles - Mechanical and electrical concepts, in ACTUATOR 2018 - 16th International Conference and Exhibition on New Actuators and Drive Systems, Conference Proceedings, 2018, pp. 514–517.

[36] SAES Smart Materials ®. SAES Getters Group, 2008, [Online]. Available: ⟨https://www.saesgetters.com/brochure-saes-smart-materials⟩.

[37] M.E. Pausley, S.J. Furst, V. Talla, S. Seelecke, Electro-mechanical behavior of a shape memory alloy actuator, Proc. SPIE - Int. Soc. Opt. Eng. 23 (2009) 783–789, https://doi.org/10.1117/12.817010

Rouven Britz completed his master's degree in mechatronics at Saarland University in 2016. Since August 2016, he has been pursuing a PhD in Systems Engineering at Saarland University, Saarbrücken, Germany. His current research focuses on shape memory wires as actuator-sensor systems in industrial applications.

Dr. Paul Motzki is the head of the research division "sensors and actuators" at the Center for Mechatronics and Automation Technology (ZeMA gGmbH) in Saarbruecken, Germany. He received his B.Sc., M.Sc. and Ph.D. degrees in Mechatronics and Systems Engineering from Saarland University, Germany. His research interests cover the design and development of multifunctional actuator-sensor-systems based on smart materials like shape memory alloys, electroactive polymers, piezo materials or magnetorheological fluids.